

# Aerodynamic-Dynamic Interactions and Multi-Body Formulation of Flapping Wing Dynamics: Part II -Trim and Stability Analysis

Ahmed M. Hassan\* and Haithem E. Taha<sup>†</sup>
University of California, Irvine, CA 92697

Flapping flight dynamics constitutes a multi-body, nonlinear, time-varying system. The two major simplifying assumptions in the analysis of flapping flight stability are neglecting the wing inertial effects and averaging the dynamics over the flapping cycle. The challenges resulting from relaxing these assumptions naturally invoke the geometric control theory as an appropriate analysis tool. In this work, a reduced-order model (extracted from the full model derived in the first part of this work) for the longitudinal flapping flight dynamics near hover is considered and represented in a geometric control framework. Then, combining tools from geometric control theory and averaging, the full dynamic stability as well as balance analyses of hovering insects are performed.

#### I. Introduction

The flight dynamics of flapping-wing micro-air-vehicles (FWMAVs) constitutes a nonlinear, time-varying, multi-body dynamical system. It is also a multi-scale dynamical system because of the associated two time scales; the time scale of the fast flapping motion and the associated aerodynamic loads, and the relatively slow time scale of the body motion. The interaction between the periodic aerodynamic loads and the body motion may induce some interesting stabilizing mechanisms [1, 2]. All of these interesting dynamical behaviors and challenges led to a recent flurry in the research on the flight dynamics of FWMAVs.

Two major assumptions are usually adopted in the flight dynamic analysis of FWMAVs [3]. These include neglecting the wing inertial effects and averaging the dynamics over the flapping cycle. The second major assumption (averaging the dynamics over the flapping cycle) has been refuted in the work of Taha et al. [1, 2] for hovering insects with a relatively small flapping frequency (e.g., hawkmoth and cranefly). They showed that in spite of the deceptive large ratio of the flapping frequency to the natural frequency of the body motion (30 for the hawkmoth and 50 for the cranefly), there is a strong interaction between the system's two time scales that considerably affects the flight stability. This interaction is essentially neglected when direct averaging is used. Thus, Taha et al. stressed the use of higher-order techniques for proper assessment of the flight stability of these insects/FWMAVs.

Considering the above two challenges (multi-body and time-varying dynamics), geometric control theory is naturally invoked as an appropriate analysis tool; the use of time-periodic inputs to generate motion in underactuated mechanical systems is a well-established concept in the arena of geometric control and averaging theory [4]. Bullo [5] considered the vibrational control of mechanical control systems by combining tools from geometric control theory and averaging. By following a similar formulation, we naturally include the wing inertial effects and the multi-body nature of FWMAVs in the analysis of their dynamics and stability. Another advantage is that higher-order averaging can be naturally performed within such a framework. Moreover, the special structure of the mechanical system along with the geometric control framework together allow for a more accurate averaging procedures (e.g., applying the variation of constants formula before averaging).

In this work, a reduced-order, three degrees-of-freedom, model (extracted from the full model derived in the first part of this work [6]) for the longitudinal flight dynamics of FWMAVs near hover is considered.

<sup>\*</sup>PhD Student, Mechanical and Aerospace Engineering. Student Member AIAA.

<sup>&</sup>lt;sup>†</sup>Assistant Professor, Henry Samueli Career Development Chair, Mechanical and Aerospace Engineering. Member AIAA.

The nonlinear, multi-body, time-varying mechanical equations are derived and represented in a geometric control framework. The combined geometric control and averaging tools are then used to derive a first-order averaged system. The stability analysis yields the first-order averaged system unstable at hover. A higher-order averaging is then used and the second-order averaged system is proven stable at hover.

## II. Reduced-order Flight Dynamic Model

In this section, a reduced-order flight dynamic model is derived from the full model considered in the first part of this work [6]. In this reduced order model we consider two degrees of freedom (DOF) for the body; the body vertical motion z and the pitching angle  $\theta$ , and one DOF for the wing; the flapping angle  $\varphi$ . The wing pitching angle  $\eta$  is assumed to have a piecewise constant variation as follows

$$\eta(t) = \begin{cases} \alpha_m, & \dot{\varphi} > 0 \\ \pi - \alpha_m, & \dot{\varphi} < 0 \end{cases},$$

where  $\alpha_m$  is the mean angle of attack over the up/down stroke. As such we have  $\sin \eta = \sin \alpha_m$  and  $\cos \eta = \cos \alpha_m \operatorname{sign}(\dot{\varphi})$ . The reduced-order model can then be written as

$$\mathcal{M}(\mathbf{q}; \operatorname{sign}(\dot{\varphi})) \ddot{\mathbf{q}} + \mathbf{f}_c(\mathbf{q}, \dot{\mathbf{q}}) = \mathbf{f}_{aero} + \mathbf{g} \tau_{\phi}, \tag{1}$$

where  $\mathcal{M}$  is the inertia matrix,  $\boldsymbol{f}_c$  represents Coriolis and centripetal effects,  $\boldsymbol{f}_{\text{aero}}$  represents the aerodynamic loads,  $\boldsymbol{g}$  is the input vector field, and  $\tau_{\phi}$  is the input torque. For the considered three-degrees-of-freedom model,  $\mathcal{M}$ ,  $\boldsymbol{f}_c$ ,  $\boldsymbol{f}_{\text{aero}}$  and  $\boldsymbol{g}$  are written as (at  $x_h = 0$ )

$$\mathcal{M} = \begin{pmatrix} m_{\rm v} & \mathcal{M}_{12} & \mathcal{M}_{13} \\ \mathcal{M}_{21} & \mathcal{M}_{22} & \mathcal{M}_{23} \\ 0 & 0 & I_{y_{\rm b}} \end{pmatrix}, \tag{2}$$

where

$$\begin{array}{rcl} \mathcal{M}_{12} & = & -r_{cg}\cos\varphi\sin\theta - \bar{c}\hat{d}\cos\alpha_{m}\,\operatorname{sign}(\dot{\varphi})\sin\varphi\sin\theta \\ \mathcal{M}_{13} & = & \bar{c}\hat{d}\cos\alpha_{m}\cos\theta\cos\varphi\,\operatorname{sign}(\dot{\varphi}) - \bar{c}\hat{d}\sin\alpha_{m}\sin\theta - r_{cg}\cos\theta\sin\varphi \\ \mathcal{M}_{21} & = & -m_{\mathbf{w}}r_{cg}\cos\varphi\sin\theta - \bar{c}\hat{d}\,m_{\mathbf{w}}\cos\alpha_{m}\,\operatorname{sign}(\dot{\varphi})\sin\varphi\sin\theta \\ \mathcal{M}_{22} & = & -\frac{1}{2}I_{x_{\mathbf{w}}}\cos^{2}\alpha_{m} - \frac{1}{2}I_{z_{\mathbf{w}}}\sin^{2}\alpha_{m} + \frac{I_{F}}{2} + \frac{I_{x_{\mathbf{w}}}+I_{z_{\mathbf{w}}}}{2} \\ \mathcal{M}_{23} & = & \frac{1}{2}(I_{z_{\mathbf{w}}} - I_{x_{\mathbf{w}}})\operatorname{sign}(\dot{\varphi})\sin2\alpha_{m}\sin\varphi \end{array}$$

$$\mathbf{f}_{c} = \begin{bmatrix}
-\dot{\theta}^{2} \left( \bar{c}\hat{d} \sin \alpha_{m} \cos \theta + \bar{c}\hat{d} \cos \alpha_{m} \sin \theta \operatorname{sign}(\dot{\varphi}) \cos \varphi - r_{cg} \sin \theta \sin \varphi \right) + \\
-2\dot{\theta}\dot{\varphi} \left( \bar{c}\hat{d} \cos \alpha_{m} \cos \theta \operatorname{sign}(\dot{\varphi}) \sin \varphi + r_{cg} \cos \theta \cos \varphi \right) + \\
+\dot{\varphi}^{2} \left( r_{cg} \sin \theta \sin \varphi - \bar{c}\hat{d} \cos \alpha_{m} \sin \theta \operatorname{sign}(\dot{\varphi}) \cos \varphi \right) - gm_{v}
\end{bmatrix}$$

$$\mathbf{f}_{c} = \begin{bmatrix}
-\dot{\theta}w \left( \bar{c}\hat{d} m_{w} \cos \alpha_{m} \cos \theta \operatorname{sign}(\dot{\varphi}) \sin \varphi + m_{w} r_{cg} \cos \theta \cos \varphi \right) + \\
+w\dot{\varphi} \left( m_{w} r_{cg} \sin \theta \sin \varphi - \bar{c}\hat{d} m_{w} \cos \alpha_{m} \sin \theta \operatorname{sign}(\dot{\varphi}) \cos \varphi \right) + \\
+\dot{\theta}^{2} \left( \frac{1}{2} \cos^{2} \alpha_{m} (I_{z_{w}} - I_{z_{w}}) \sin \varphi \cos \varphi + \frac{1}{2} \sin^{2} \alpha_{m} (I_{x_{w}} - I_{z_{w}}) \sin \varphi \cos \varphi + \\
+\frac{1}{2} (-I_{x_{w}} - I_{z_{w}}) \sin \varphi \cos \varphi + \frac{1}{2} I_{y_{w}} \sin 2\varphi \right)$$
(3)

0

$$\boldsymbol{f}_{\text{aero}} = \begin{bmatrix} -F_x \left( \sin \alpha_m \cos \theta + \cos \alpha_m \sin \theta \, \operatorname{sign}(\dot{\varphi}) \cos \varphi \right) - F_z \left( \sin \alpha_m \sin \theta \cos \varphi - \cos \alpha_m \cos \theta \, \operatorname{sign}(\dot{\varphi}) \right) \\ \sin \alpha_m M_x - \cos \alpha_m M_z \, \operatorname{sign}(\dot{\varphi}) \\ -\cos \alpha_m M_x \, \operatorname{sign}(\dot{\varphi}) \sin \varphi + M_y \cos \varphi - \sin \alpha_m M_z \sin \varphi \end{bmatrix}$$

$$(4)$$

$$\mathbf{g} = \begin{bmatrix} 0 \\ 1 \\ 0 \end{bmatrix}, \tag{5}$$

where  $F_x$ ,  $F_z$ ,  $M_x$ ,  $M_y$ , and  $M_z$  are the aerodynamic forces and moments represented in the wing frame as explained in the first part of this work,  $I_F$  is the flapping moment of inertia defined as  $I_F = I_{x_w} \sin^2 \alpha_m + I_{z_w} \cos^2 \alpha_m$ ,  $\bar{c}$  is the mean aerodynamic chord of the wing, and  $\hat{d}$  and  $r_{cg}$  are the distances from the wing reference point to the wing center of mass along  $x_w$  and  $y_w$  respectively.

In order for this model to be in a form that is amenable to geometric control analysis, we write it in a standard nonlinear control-affine system form. As such, system (1) can be written as

$$\dot{\boldsymbol{x}} = \boldsymbol{Z}(\boldsymbol{x}) + \boldsymbol{Y}(\boldsymbol{x}) \ \tau_{\varphi}(t), \tag{6}$$

where the state vector  $\boldsymbol{x}$  is  $[\boldsymbol{q} \quad \dot{\boldsymbol{q}}]^T = [z \quad \varphi \quad \theta \quad w \quad \dot{\varphi} \quad \dot{\theta}]^T$ , T denotes transpose, and the vector fields  $\boldsymbol{Z}(\boldsymbol{x})$  and  $\boldsymbol{Y}(\boldsymbol{x})$  are written as

$$m{Z}(m{x}) = egin{bmatrix} \dot{m{q}} \ \mathcal{M}^{-1}(m{f}_{ ext{aero}} - m{f}_c) \end{bmatrix}, \qquad m{Y}(m{x}) = egin{bmatrix} m{0} \ \mathcal{M}^{-1}m{g} \end{bmatrix},$$

The input torque applied on the wings is assumed to be periodic of a cosine wave form with frequency  $\omega$  and amplitude U

$$\tau_{\varphi}(t) = U \cos \omega t. \tag{7}$$

## III. Geometric Control and Averaging Tools

#### A. Averaging Theorem

**Theorem 1.** Consider the NLTP system

$$\dot{\boldsymbol{x}}(t) = \epsilon \boldsymbol{X}(\boldsymbol{x}(t), t). \tag{8}$$

Assuming that X is a T-periodic vector field in t, the averaged dynamical system corresponding to (8) is written as

$$\dot{\overline{x}} = \epsilon \overline{X}(\overline{x}), \tag{9}$$

where  $\overline{\boldsymbol{X}}(\overline{\boldsymbol{x}}) = \frac{1}{T} \int_0^T \boldsymbol{X}(\boldsymbol{x}, \tau) d\tau$ . According to the averaging theorem [8], [9]:

- If  $\boldsymbol{x}(0) \overline{\boldsymbol{x}}(0) = O(\epsilon)$ , then there exist  $b \in \mathbb{R}_{>0}$  and  $\epsilon^* \in \mathbb{R}_{>0}$  such that  $\boldsymbol{x}(t) \overline{\boldsymbol{x}}(t) = O(\epsilon) \ \forall t \in [0, b/\epsilon]$  and  $\forall \epsilon \in [0, \epsilon^*]$ .
- If the origin  $\overline{x} = 0$  is an exponentially stable equilibrium point of (9) and if  $x(0) \overline{x}(0) = O(\epsilon)$ , then there exists an  $\epsilon^*$  such that  $x(t) \overline{x}(t) = O(\epsilon) \ \forall t > 0$  and  $\forall \epsilon \in [0, \epsilon^*]$ . Moreover, The system (8) has a unique, exponentially stable, T-periodic solution  $x_T(t)$  with the property  $||x_T(t)|| \le k\epsilon$  for some k.

Thus, the averaging approach allows converting a non-autonomous system into an autonomous system. As such, if the equilibrium state of the NLTP system is represented by a periodic orbit  $x^*(t)$ , it reduces to a fixed point of the averaged dynamics. The problem of ensuring a specific periodic orbit corresponding to a desired equilibrium configuration is significantly simplified using the averaging approach, hence allowing for analytical results. Suppose the system is characterized by a vector of parameters P (e.g., U in our three DOF

FWMAV example) and denote this parametric dependence as follows:  $X(x, t; \mathbf{P})$ . Without loss of generality, assume that it is required to ensure a periodic orbit  $x^*(t)$  with zero-mean (e.g., hovering equilibrium in our three DOF FWMAV example). Hence, the balance problem is stated as follows: Determine the system parameters  $\mathbf{P}$  and the periodic orbit  $x^*(t)$  such that

$$\dot{\boldsymbol{x}}^*(t) = \boldsymbol{X}(\boldsymbol{x}^*(t), t; \boldsymbol{P}),$$

with  $\overline{x}^* = \mathbf{0}$ . Obviously, it is not a trivial problem and often cannot be solved analytically. In contrast, the balance problem using the averaging approach is stated as follows: Determine the system parameters P that are necessary to ensure  $\overline{X}(0; P) = \mathbf{0}$ . This is achieved by solving a set of algebraic equations.

One caveat we should mention before leaving this point is that the averaging theorem requires the vector field  $\mathbf{X}(\mathbf{x}(t),t)$  to be smooth in all its arguments. Unfortunately, the dynamics vector field,  $\mathbf{Z}$ , in system (6) is not smooth in the state  $\dot{\varphi}$  because of the absolute value function,  $|\dot{\varphi}|$ . We tackle this issue by introducing a smooth approximation for the absolute value function. For more details about this point, the reader is referred to an earlier work by Taha et al. [10].

## B. Generalized Averaging Theory

A main issue with the averaging approach is that it is valid for small enough  $\epsilon$  (i.e., for high enough frequency). Moreover, this frequency limit (determined by  $\epsilon^*$ ) is not known (only its existence is guaranteed). The generalized averaging theory (GAT) presents a remedy for this issue by providing an arbitrarily higher-order approximation to the flow along a time-periodic vector field. Agrachev and Gamkrelidze laid the foundation for the GAT in their seminal work [11]. Later, Sarychev [12] and Vela [13] used the concepts introduced by Agrachev and Gamkrelidze to develop a generalization for the classical averaging theorem. Only the final results of the GAT are stated here, and the reader is referred to Section 4 in [2] for a detailed presentation of the GAT. Sarychev [12] introduced the notion of complete averaging to denote the following averaged dynamics of system (8)

$$\dot{\bar{x}} = \epsilon \bar{X} = \epsilon \Lambda_1(\bar{x}) + \epsilon^2 \Lambda_2(\bar{x}) + \epsilon^3 \Lambda_3(\bar{x}) + ..., \tag{10}$$

where

$$\Lambda_{1}(\bar{\boldsymbol{x}}) = \frac{1}{T} \int_{0}^{T} \boldsymbol{X}(\boldsymbol{x}, t) dt$$

$$\Lambda_{2}(\bar{\boldsymbol{x}}) = \frac{1}{2T} \int_{0}^{T} \left[ \int_{0}^{t} \boldsymbol{X}(\boldsymbol{x}, \sigma) d\sigma, \, \boldsymbol{X}(\boldsymbol{x}, t) \right] dt$$

$$\Lambda_{3}(\bar{\boldsymbol{x}}) = \frac{T}{2} \left[ \Lambda_{1}(\bar{\boldsymbol{x}}), \, \Lambda_{2}(\bar{\boldsymbol{x}}) \right] + \frac{1}{3T} \int_{0}^{T} \left[ \int_{0}^{t} \boldsymbol{X}(\boldsymbol{x}, \sigma) d\sigma, \left[ \int_{0}^{t} \boldsymbol{X}(\boldsymbol{x}, \sigma) d\sigma, \boldsymbol{X}(\boldsymbol{x}, t) \right] \right] dt,$$
(11)

where the Lie bracket between two vector fields is defined as  $[V_1(x), V_2(x)] = \frac{\partial V_2}{\partial x} V_1 - \frac{\partial V_1}{\partial x} V_2$ . Sarychev and Vela showed that if the series (10) converges, its limit will be the logarithm of the Monodromy map (i.e., the nonlinear vector-valued function that maps an initial condition to the solution after the period T). That is, if the complete averaged dynamics (10) has an exponentially stable fixed point, then the NLTP system (8) will have an exponentially stable periodic orbit, irrespective of  $\epsilon$ .

## C. Variation of Constants Formula (VOC)

Variation of constants formula is quite useful when the concerned nonlinear system is subjected to high-amplitude periodic forcing. In such cases, the system is not even directly amenable to the averaging theorem. Consider a nonlinear system subjected to a high-frequency, high-amplitude, periodic forcing in the form

$$\dot{\boldsymbol{x}} = \boldsymbol{f}(\boldsymbol{x}) + \frac{1}{\epsilon} \boldsymbol{g}(\boldsymbol{x}, \ \frac{t}{\epsilon}), \qquad \boldsymbol{x}(0) = \boldsymbol{x}_0, \tag{12}$$

where  $0 < \epsilon \ll 1$ . The time-varying vector field  $g(x, t/\epsilon)$  is assumed to be periodic in its second argument with period T. The system (12) is not even amenable to direct averaging, i.e., is not in the form of (8), because f and g are not of the same order. The VOC formula allows separation of the system (12) into two companion systems as follows [11], [14]

$$\dot{z} = F(z,t), \quad z(0) = x_0 
\dot{x} = g(x,t), \quad x(0) = z(t),$$
(13)

where F(x,t) is the *pullback* of f along the flow  $\phi_t^{g}$  of the time-varying vector field g. Using the chronological calculus formulation of Agrachev and Gamkrelidze [11], Bullo [15] showed that, for a time-invariant f and time-varying g, the pullback vector field F(x,t) can be written as

$$\mathbf{F}(\mathbf{x},t) = \mathbf{f}(\mathbf{x}) + \sum_{k=1}^{\infty} \int_{0}^{t} \dots \int_{0}^{s_{k-1}} \left( ad\mathbf{g}(S_{k},\mathbf{x}) \dots ad\mathbf{g}(S_{1},\mathbf{x}) \mathbf{f}(\mathbf{x}) \right) ds_{k} \dots ds_{1},$$
(14)

where adg f = [g, f]. Now, if the vector field g is T-periodic in t with zero mean, the averaging of system (13) yields

$$\bar{\boldsymbol{x}}(t) = \bar{\boldsymbol{z}}(t), \quad \dot{\bar{\boldsymbol{z}}} = \bar{\boldsymbol{F}}(\bar{\boldsymbol{z}}).$$
 (15)

Hence, in this case, one can recover the averaged dynamics of the original system (12) just by applying the averaging on the pullback vector field F(x,t).

## D. First Order Averaging after VOC

**Theorem 2.** Consider a NLTP system subject to a high-frequency, high amplitude, periodic forcing (12). Assuming that g is a T-periodic in t, zero-mean, vector field and both f and g are continuously differentiable, the averaged dynamical system corresponding to (12) is written as

$$\dot{\overline{x}} = \epsilon \overline{F}(\overline{x}), \tag{16}$$

where  $\overline{F}(\overline{x}) = \frac{1}{T} \int_0^T F(x, \tau) d\tau$ , and F is the pullback of f along the flow  $\phi_t^{g}$  of the time-varying vector field g as explained in Eq. (14). Moreover [14]:

- If  $\overline{x}(0) = x(0)$ , then there exist  $b \in \mathbb{R}_{>0}$  and  $\epsilon^* \in \mathbb{R}_{>0}$  such that  $x(t) \overline{x}(t) = O(\epsilon) \ \forall t \in [0, b/\epsilon]$  and  $\forall \epsilon \in [0, \epsilon^*]$ .
- If  $\boldsymbol{x}^*$  is an exponentially stable equilibrium point of (16) and if  $\|\boldsymbol{x}(0) \boldsymbol{x}^*\| < \rho$  for some  $\rho \in \mathbb{R}_{>0}$ , then  $\boldsymbol{x}(t) \overline{\boldsymbol{x}}(t) = O(\epsilon) \ \forall t > 0$  and  $\forall \epsilon \in [0, \epsilon^*]$ . Moreover, there exists an  $\epsilon_1 \in \mathbb{R}_{>0}$  such that  $\forall \epsilon \in [0, \epsilon_1]$ , the system (12) has a unique,  $\epsilon T$ -periodic, locally asymptotically stable trajectory that takes values in an open ball of radius O(1) centered at  $\boldsymbol{x}^*$ .

## IV. Averaging of the Three-DOF Time-varying Dynamics

Clearly, the direct application of the averaging theorem to the system (6), with  $\tau_{\varphi}$  given by (7), yields trivial results (i.e., no effect of flapping on the dynamics). Hence, we apply the VOC formula before averaging to obtain the pullback vector field which accounts for the effect of the forcing vector field on the dynamics (drift) vector filed. That is, the averaged dynamics will be determined from (15). Thanks to the mechanical structure of the system (6) and because the non-conservative forces (aerodynamic loads) are quadratic in the generalized velocities  $(w, \dot{\varphi}, \text{ and } \dot{\theta})$ , the integral series of the pullback vector field (14) terminates after two terms. Hence, the pullback vector field of the system (6) can be written as

$$F(x,t) = Z(x) + [Y, Z] \int_{0}^{t} \tau_{\varphi}(s_{1}) ds_{1} + [Y, [Y, Z]] \int_{0}^{t} \int_{0}^{s_{1}} \tau_{\varphi}(s_{2}) \tau_{\varphi}(s_{1}) ds_{2} ds_{1}.$$
 (17)

## A. VOC Formula with First Order Averaging

In order to obtain the first term,  $\Lambda_1(\bar{x})$ , in the averaging series; i.e., a first-order averaged system, we apply the definition of  $\Lambda_1(\bar{x})$  as shown in Eq. (11) on the pullback vector field (17). Since the control input torque is represented as a cosine-wave form, the coefficient of the first Lie bracket in (17), [Y, Z], vanishes after the first order averaging. Hence, the first-order averaged system is written as

$$\dot{\bar{x}} = \Lambda_1(\bar{x}) = Z(\bar{x}) + \frac{U^2}{4 \omega^2} [Y, [Y, Z]] (\bar{x}), \tag{18}$$

where the Lie bracket [Y, [Y, Z]] is called the *symmetric product* of the control vector field Y. It should be noted that the symmetric product preserves the mechanical structure of the system, hence the mechanical structure is preserved under the VOC formula with first order averaging.

In order to achieve balance at hovering, we solve for the appropriate control input torque amplitude,  $U_{trim}$  that ensures  $\Lambda_1(\bar{x}) = 0$ . As such, we obtain

$$U_{trim} = \sqrt{\frac{2 g I_F^2 \omega^2}{k_L}},\tag{19}$$

where  $k_L$  is a constant that depends on the vehicle parameters

$$k_L = \frac{\rho \ C_{L_{\alpha}} I_{21} \sin \alpha_m \cos \alpha_m}{2 \ m_{\text{v}}}.$$

It should be noted that for trim and stability analysis we adopted a smooth approximation for the sign function;  $\operatorname{sign}(\dot{\varphi}) \approx h(\dot{\varphi}) = (2/\pi) \tan^{-1}(n \dot{\varphi})$ . We set an appropriate value of n such that, in 1% of the  $\dot{\varphi}$  range around the origin, the approximate function  $h(\dot{\varphi})$  reaches 99% of the true value (±1).

The stability of the averaged system can be scrutinized by evaluating the Jacobian of the averaged dynamics at the trim condition which can be written as

$$\mathbf{A} = D \; \mathbf{\Lambda}_{1}(\mathbf{0}) = \begin{bmatrix} 0 & 0 & 0 & 1 & 0 & 0 \\ 0 & 0 & 0 & 0 & 1 & 0 \\ 0 & 0 & 0 & 0 & 0 & 1 \\ 0 & 0 & 0 & A_{44} & 0 & 0 \\ 0 & 0 & A_{53} & 0 & A_{55} & 0 \\ 0 & A_{62} & A_{63} & 0 & A_{65} & A_{66} \end{bmatrix}, \tag{20}$$

where

$$\begin{array}{rcl} A_{44} & = & \frac{g - \cos \alpha_m}{I_{21} \sin \alpha_m} \left( \frac{-23}{2} I_{11} + \frac{46 \ m_{\rm w} \bar{c} d}{I_{y_{\rm b}}} \left( \frac{3}{4} I_{12} - k \ I_{11} \right) \right) \\ A_{53} & = & -2 \ g \ m_{\rm v} m_{\rm w} r_{cg} \\ A_{55} & = & -\rho \ C_{L_{\alpha}} \sin^2 \alpha_m \ I_{21} / I_F \\ A_{62} & = & 2 \ g \ m_{\rm v} I_{31} / (I_{y_{\rm b}} I_{21}) \\ A_{63} & = & \frac{-2 \ g \ m_{\rm w} r_{cg}}{I_{y_{\rm b}} I_{21} \sin \alpha_m} \left( \frac{3}{4} I_{12} - k \ I_{11} \right) \\ A_{65} & = & \frac{-69 \ g \ m_{\rm v}}{I_{y_{\rm b}} I_{21} \cos \alpha_m} \left( \frac{3}{4} I_{22} - k \ I_{21} \right) \\ A_{66} & = & \frac{-23 \ g \ m_{\rm v} \pi}{8 \ I_{y_{\rm b}} I_{21} C_{L_{\alpha}} \cos \alpha_m} \left( 4 \ k \ I_{12} - 4 \ k^2 I_{11} - \frac{3}{4} I_{13} \right) \end{array}$$

It should be noted that the elements  $A_{63}$  and  $A_{66}$  represent the pitch stiffness and damping respectively. Hence, they are of particular interest as the unstable behavior signifies mainly in the body pitching motion.

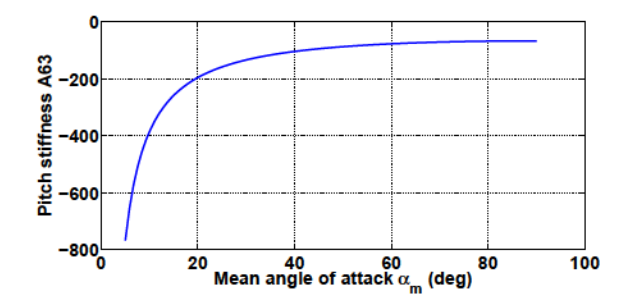
If we consider the Hawkmoth parameters given in Appendix A, we find that the pitch stiffness  $A_{63} = -133.99$ , hence a positive pitch stiffness. It should be noted that this pitch stiffness stems purely from an inertial root; i.e.,

$$\lim_{m_{\rm w} \to 0} A_{63} = 0.$$

It is interesting to investigate the main contributors to this pitch stiffness. Since the averaged dynamics is written in terms of two vector fields; the dynamics vector field and the symmetric product, or we shall call it the control vector field, as explained in Eq. (18), thus this Jacobian matrix  $\mathbf{A}$  can be seen as an addition of two matrices  $\mathbf{A}_d$  and  $\mathbf{A}_c$  and the effect emanating from each source can shown separately. Doing so, we find that  $A_{d_{63}} = 0$ , hence the pitch stiffness comes solely from the control effect. This also implies that the high-frequency-high-amplitude periodic forcing applied on the wing has a stabilizing effect on the body pitching motion. It is also interesting to observe the variation of the pitch stiffness,  $A_{63}$ , with the mean angle of attack over the up/down stroke  $\alpha_m$ . Figure 1 shows the variation of the pitch stiffness of the averaged system,  $A_{63}$ , as the mean angle of attack varies from zero to 90°.

The pitch damping,  $A_{66}$ , for the Hawkmoth is found to be  $A_{66} = -607.5$ , hence a positive pitch damping. It should be noted that the pitch damping emanates from inertial as well as aerodynamic sources. Following

the same analysis we performed for the pitch stiffness, we find that  $A_{dee} = 0$ , hence the pitch damping also comes solely from the control effect. This also implies the stabilizing pitch damping effect induced by the high-frequency-high-amplitude periodic forcing applied on the wings. Figure 2 shows the variation of the pitch damping of the averaged system,  $A_{66}$ , as the mean angle of attack varies from zero to 90°.



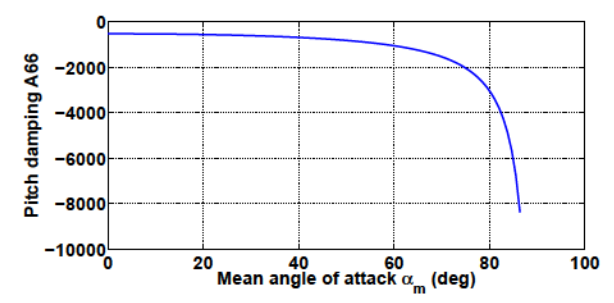


Figure 1: Pitch stiffness variation with the mean angle of attack.

Figure 2: Pitch damping variation with the mean angle of attack.

The stability of the considered time-periodic system (1), or equivalently (6), can be assessed by investigating the eigenvalues of the linearized averaged system (20) which are found to be

$$-6419.27$$
,  $-554.009$ ,  $-204.819$ ,  $141.508$ ,  $0.232108$ 

Clearly the averaged system is unstable since there are two eigenvalues in the right half-plane. However, since it has been shown before that the higher-order averaging analysis might yield different stability results for the FWMAVs [2], it is expected that applying higher-order averaging after VOC formula for the multi-body formulation considered here might also yield different results. This invokes including more terms from the averaging series defined in Eq. (10) which is considered in the next subsection.

## B. VOC Formula with Second Order Averaging

The second term in the averaging series  $\Lambda_2(\bar{x})$  can be obtained from the pullback vector field (17) as explained in Eq. (11), and it can be written as (under cosine wave form)

$$\Lambda_2(\bar{x}) = \frac{-U}{\omega^2} [Z, [Y, Z]] (\bar{x}) + \frac{U^3}{4 \omega^4} [[Y, Z], [Y, [Y, Z]]] (\bar{x}), \tag{21}$$

Hence, the second-order averaged dynamics can be written as

$$\dot{\bar{x}} = \Lambda_1(\bar{x}) + \Lambda_2(\bar{x}) = Z(\bar{x}) + \frac{U^2}{4\omega^2} [Y, [Y, Z]](\bar{x}) + \frac{-U}{\omega^2} [Z, [Y, Z]](\bar{x}) + \frac{U^3}{4\omega^4} [[Y, Z], [Y, [Y, Z]]](\bar{x}). \tag{22}$$

Unfortunately, the second-order averaged dynamics (22) does have Lie brackets that ruin the mechanical structure of the system. Hence, the trim analysis is more involved since the first three equations in (22) are not trivial anymore; i.e., there might be an equilibrium at non-zero  $\dot{\varphi}$ . Due to the system complexity, in particular, the existence of the sign function, we could not be able to perform the trim analysis at non-zero  $\dot{\varphi}$ . If a zero-average state vector is considered for the trim analysis, solving for the appropriate control input torque amplitude,  $U_{trim}$ , yields the same result as that of the first-order averaging given in (19). Hence, the second-order averaging does not add new information to the balance problem.

To assess the stability of the second-order averaged dynamics, we investigate its linearization as follows

$$A_{2nd} = D \left( \Lambda_1 + \Lambda_2 \right) (0) = \begin{bmatrix} 0 & 0 & A_{2nd_{13}} & 1 & A_{2nd_{15}} & 0 \\ 0 & 0 & 0 & A_{2nd_{24}} & 1 & 0 \\ 0 & 0 & 0 & A_{2nd_{34}} & 0 & 1 \\ 0 & A_{2nd_{42}} & A_{2nd_{43}} & A_{2nd_{44}} & A_{2nd_{45}} & A_{2nd_{46}} \\ 0 & 0 & A_{2nd_{53}} & A_{2nd_{54}} & A_{2nd_{55}} & 0 \\ 0 & A_{2nd_{62}} & A_{2nd_{63}} & A_{2nd_{64}} & A_{2nd_{65}} & A_{2nd_{66}} \end{bmatrix},$$
(23)

where

$$\begin{array}{lll} A_{2nd_{13}} & = & \frac{\sqrt{\frac{g}{k_L}}}{I_F m_{\nu} \omega} \left( \sqrt{2} \ \rho \ C_{L_{\alpha}} \sin^2 \alpha_m I_{21} \ m_{\rm w} r_{cg} - \frac{23}{\sqrt{2}} m_{\rm w} \bar{c} \hat{d} \sin \alpha_m \ \frac{gI_F}{k_L} \right) \\ A_{2nd_{15}} & = & \frac{2\sqrt{2k_L g}}{\omega} \\ A_{2nd_{24}} & = & \frac{1}{I_F \ \omega} \ \rho \ C_{L_{\alpha}} \sin \alpha_m \cos \alpha_m I_{21} \sqrt{\frac{2g}{k_L}} \\ A_{2nd_{34}} & = & \frac{1}{I_{y_b} \omega} \ \rho \ C_{L_{\alpha}} \cos \alpha_m \left( \frac{3}{4} I_{12} - k \ I_{11} \right) \sqrt{\frac{2g}{k_L}} \\ A_{2nd_{44}} & = & A_{44} \\ A_{2nd_{53}} & = & A_{53} \\ A_{2nd_{55}} & = & A_{55} \\ A_{2nd_{62}} & = & A_{62} \\ A_{2nd_{63}} & = & A_{63} \\ A_{2nd_{65}} & = & A_{65} \\ A_{2nd_{66}} & = & A_{66} \end{array}$$

The rest of the derivatives have too lengthy expressions. Thus, we show here the limits as  $m_{\rm w}$  goes to zero

$$\begin{split} &\lim_{m_{\mathrm{w}}\to 0} A_{2nd_{42}} &= \frac{-1}{m_{\mathrm{b}}I_{y_{\mathrm{b}}}\omega}\sqrt{2}\; (\frac{g}{k_{L}})^{3/2}\; \pi \rho^{2}C_{L_{\alpha}}\sin\alpha_{m}\cos\alpha_{m}I_{31}\left(k\frac{I_{11}}{2}-\frac{I_{12}}{8}\right) \\ &\lim_{m_{\mathrm{w}}\to 0} A_{2nd_{43}} &= \frac{69\sqrt{2}}{4\;m_{\mathrm{b}}I_{F}\omega}(\frac{g}{k_{L}})^{3/2}\rho^{2}\;C_{L_{\alpha}}^{2}\sin^{4}\alpha_{m}I_{21}^{2} \\ &\lim_{m_{\mathrm{w}}\to 0} A_{2nd_{45}} &= \frac{\rho C_{L_{\alpha}}\sqrt{\frac{g}{k_{L}}}}{\sqrt{2}\;m_{\mathrm{b}}I_{y_{\mathrm{b}}}\omega}\left(-23\;\cos^{2}\alpha_{m}\;g\;I_{11}+69\pi\rho\sin\alpha_{m}\frac{g}{k_{L}}\left(\frac{3}{4}I_{22}-kI_{21}\right)\left(k\frac{I_{11}}{2}-\frac{I_{12}}{8}\right)\right) \\ &\lim_{m_{\mathrm{w}}\to 0} A_{2nd_{46}} &= \frac{1}{4\sqrt{2}\;I_{F}I_{y_{\mathrm{b}}}}\sqrt{\frac{g}{k_{L}}}\pi\rho^{2}\;C_{L_{\alpha}}\sin^{2}\alpha_{m}I_{21}\left(kI_{11}-\frac{I_{12}}{4}\right)\left(-4I_{y_{\mathrm{b}}}+23g\frac{I_{F}}{k_{L}}\right) + \\ &\quad - \frac{23}{4\sqrt{2}\;m_{\mathrm{b}}^{2}\omega}\left(\frac{g}{k_{L}}\right)^{3/2}\;\pi\rho^{2}\;C_{L_{\alpha}}\cos^{2}\alpha_{m}I_{11}\left(kI_{11}-\frac{I_{12}}{4}\right) \end{split}$$

 $A_{2nd_{54}}$  and  $A_{2nd_{64}}$  have too lengthy expressions even after taking the limits as  $m_{\rm w}$  goes to zero. Thus, we just mention the signs of these derivatives here;  $A_{2nd_{54}}$  has a positive value and  $A_{2nd_{64}}$  has a negative value. It is interesting to notice that the pitch stiffness and damping represented by  $A_{2nd_{63}}$  and  $A_{2nd_{66}}$  respectively, among other derivatives, did not change after including the second term in the averaging series. Equation (24) shows the first and second order averaged systems Jacobians for the Hawkmoth case. The stability of the second-order averaged system (22) can be assessed by investigating the eigenvalues of the linearization (23) which are found to be (for the Hawkmoth case)

$$-3217.85 \pm 7253.1 \ i, -500.733, -99.68, -0.24$$

It is noted that all the eigenvalues lie in the left half-plane. According to Lyapunov's first method [16], the nonlinear averaged system (22) is concluded locally asymptotically stable. Figure 3 shows the eigenvalues of

the first and second-order linearized averaged systems together on the s-plane.

$$\mathbf{A}_{1st} = \begin{bmatrix}
0 & 0 & 0 & 1 & 0 & 0 \\
0 & 0 & 0 & 0 & 1 & 0 \\
0 & 0 & 0 & 0 & 0 & 1 \\
0 & 0 & 0 & -6419.27 & 0 & 0 \\
0 & 0 & -616.406 & 0 & -9.57 & 0 \\
0 & 6046.32 & -133.992 & 0 & -26053.9 & -607.518
\end{bmatrix}$$

$$\mathbf{A}_{2nd} = \begin{bmatrix}
0 & 0 & 0.024 & 1 & 0.0013 & 0 \\
0 & 0 & 0 & 17.82 & 1 & 0 \\
0 & 0 & 0 & 3.87 & 0 & 1 \\
0 & -648.258 & 1544.16 & -6419.27 & -3.2116 & 15.087 \\
0 & 0 & -616.406 & 78611.3 & -9.57 & 0 \\
0 & 6046.32 & -133.992 & -4.15273 * 10^6 & -26053.9 & -607.518
\end{bmatrix}$$
(24)

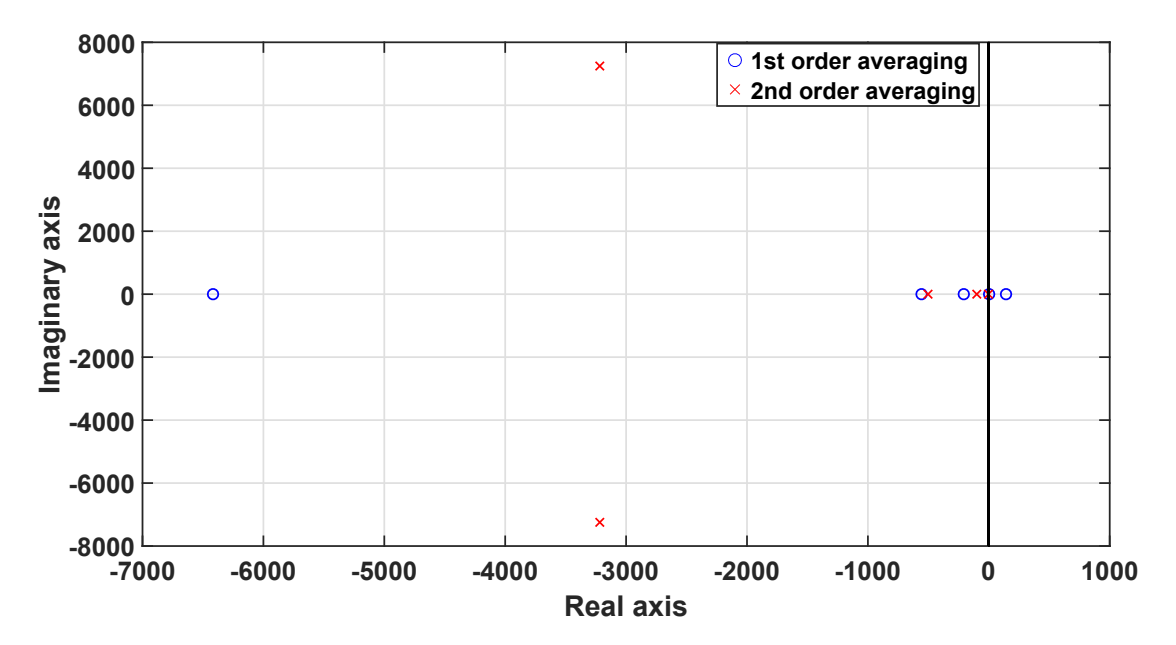


Figure 3: Eigenvalues of the first and second-order averaged linearized systems with the Hawkmoth parameters.

## V. Conclusion

The longitudinal fight dynamics of flapping-wing micro-air-vehicles (FWMAVs)/insects is considered. A reduced-order, three-DOF, multi-body model extracted from the full five-DOF dynamics is considered. In order to rigorously and analytically analyze the balance problem and assess the longitudinal flight stability near hover, while including the wing inertial effects, the geometric control theory and averaging are combined. Applying VOC formula before averaging yielded an unstable averaged system. As a vibrational stabilization effect is anticipated, we applied second-order averaging after VOC formula. The resulting second-order averaged system has been proven stable, hence a stable time-periodic dynamics.

# Appendix

## A. Hawkmoth Morphological Parameters

The morphological parameters and the wing planform for the hawkmoth, as given in [17] and [18], are

$$R = 51.9 \text{mm}, \text{ S} = 947.8 \text{mm}^2, \ \overline{c} = 18.3 \text{mm},$$
  
 $\hat{r}_1 = 0.44, \ \hat{r}_2 = 0.525, \ f = 26.3 \text{Hz}, \ \Phi = 60.5^{\circ},$   
 $\alpha_m = 30^{\circ}, \ m_b = 1.648 \text{gm}, \ \text{and} \ \text{I}_{\text{vb}} = 2080 \text{mg.cm}^2,$ 

where R is the semi-span of the wing, S is the area of one wing,  $\bar{c}$  is the mean chord, f is the flapping frequency,  $\Phi$  is the flapping angle amplitude,  $m_b$  is the mass of the body, and  $I_{yb}$  is the body moment of inertia around the body y-axis. The moments of the wing chord distribution  $\hat{r}_1$  and  $\hat{r}_2$  are defined as

$$I_{k1} = 2 \int_0^R r^k c(r) \, dr = 2SR^k \hat{r}_k^k.$$

As for the wing planform, the method of moments used by Ellington [18] is adopted here to obtain a chord distribution for the insect that matches the documented first two moments  $\hat{r}_1$  and  $\hat{r}_2$ ; that is,

$$c(r) = \frac{\overline{c}}{\beta} \left(\frac{r}{R}\right)^{\lambda - 1} \left(1 - \frac{r}{R}\right)^{\gamma - 1},$$

where

$$\lambda = \hat{r}_1 \left[ \frac{\hat{r}_1 (1 - \hat{r}_1)}{\hat{r}_2^2 - \hat{r}_1^2} - 1 \right] , \ \gamma = (1 - \hat{r}_1) \left[ \frac{\hat{r}_1 (1 - \hat{r}_1)}{\hat{r}_2^2 - \hat{r}_1^2} - 1 \right],$$
 and  $\beta = \int_0^1 \hat{r}^{\lambda - 1} (1 - \hat{r})^{\gamma - 1} d\hat{r}.$ 

The mass of one wing is taken as 5.7% of the body mass according to Wu et al. [19] and is assumed uniform with an areal mass distribution m' The inertial properties of the wing are then estimated as

$$\begin{split} I_x &= 2 \int_0^R m' r^2 c(r) \, dr \;, \; I_y = 2 \int_0^R m' \hat{d}^2 c^3(r) \, dr \\ , I_z &= I_x + I_y, \; \text{and} \; r_{\text{cg}} = \frac{2 \int_0^R m' r c(r) \, dr}{m_{\text{w}}} = \frac{I_{11}}{2S}, \end{split}$$

where  $\hat{d}$  is the chord-normalized distance from the wing hinge line to the center of gravity line.

# Acknowledgments

The authors gratefully acknowledge the support of the National Science Foundation grants CMMI-1435484 and CMMI-1709746, and program manager Dr. Jordan Berg.

## References

- <sup>1</sup> Taha, H. E., Nayfeh, A. H., and Hajj, M. R., "Effect of the aerodynamic-induced parametric excitation on the longitudinal stability of hovering MAVs/insects," *Nonlinear Dynamics*, Vol. 78, No. 4, 2014, pp. 2399–2408.
- <sup>2</sup> Taha, H. E., Tahmasian, S., Woolsey, C. A., Nayfeh, A. H., and Hajj, M. R., "The need for higher-order averaging in the stability analysis of hovering, flapping-wing flight," *Bioinspiration & biomimetics*, Vol. 10, No. 1, 2015, pp. 016002.
- <sup>3</sup> Taha, H. E., Hajj, M. R., and Nayfeh, A. H., "Flight Dynamics and Control of Flapping-Wing MAVs: A Review," *Nonlinear Dynamics*, Vol. 70, No. 2, 2012, pp. 907–939.
- <sup>4</sup> Bullo, F. and Lewis, A. D., *Geometric control of mechanical systems*, Applied Mathematics, Springer-Verlag, Berlin, Germany, 2004.
- <sup>5</sup> Bullo, F., "Averaging and vibrational control of mechanical systems," SIAM Journal on Control and Optimization, Vol. 41, No. 2, 2002, pp. 542–562.

- <sup>6</sup> Hassan, A. M. and Taha, H. E., "Aerodynamic-Dynamic Interactions and Multi-Body Formulation of Flapping Wing Dynamics: Part I - Modeling," AIAA Guidance, Navigation, and Control Conference, 2017.
- Agrachev, A. A. and Gamkrelidze, R. V., "The exponential representation of flows and the chronological calculus," *Mathematics of the USSR: Sbornik*, Vol. 35, No. 6, 1979, pp. 727–785.
- <sup>8</sup> Guckenheimer, J. and Holmes, P., Nonlinear oscillations, dynamical systems, and bifurcations of vector fields, Vol. 42, Springer Science & Business Media, 2013.
- <sup>9</sup> Sanders, J. A., Verhulst, F., and Murdock, J. A., Averaging methods in nonlinear dynamical systems, Vol. 59, Springer, 2007.
- Taha, H. E., Woolsey, C. A., and Hajj, M. R., "Geometric Control Approach to Longitudinal Stability of Flapping Flight," *Journal of Guidance, Control, and Dynamics*, Vol. 39, No. 2, 2016, pp. 214–226.
- <sup>11</sup> Agrachev, A. A. and Gamkrelidze, R. V., "The exponential representation of flows and the chronological calculus," *Matematicheskii Sbornik*, Vol. 149, No. 4, 1978, pp. 467–532.
- Sarychev, A., "Stability criteria for time-periodic systems via high-order averaging techniques," Nonlinear control in the year 2000 volume 2, Springer, 2001, pp. 365-377.
- Vela, P. A., Averaging and control of nonlinear systems, Ph.D. thesis, California Institute of Technology, 2003.
- <sup>14</sup> Bullo, F. and Lewis, A. D., Geometric control of mechanical systems: modeling, analysis, and design for simple mechanical control systems, Vol. 49, Springer Science & Business Media, 2004.
- <sup>15</sup> Bullo, F., "Averaging and vibrational control of mechanical systems," SIAM Journal on Control and Optimization, Vol. 41, No. 2, 2002, pp. 542–562.
- <sup>16</sup> Khalil, H. K., Nonlinear Systems, Prentice Hall, 3rd ed., 2002.
- <sup>17</sup> Sun, M., Wang, J., and Xiong, Y., "Dynamic Flight Stability of Hovering Insects," Acta Mechanica Sinica, Vol. 23, No. 3, 2007, pp. 231–246.
- <sup>18</sup> Ellington, C. P., "The aerodynamics of hovering insect flight: II. Morphological parameters," *Philosophical Transactions Royal Society London Series B*, Vol. 305, 1984, pp. 17–40.
- Wu, J. H., Zhang, Y. L., and Sun, M., "Hovering of model insects: simulation by coupling equations of motion with Navier-Stokes equations," *The Journal of Experimental Biology*, Vol. 212, No. 20, 2009, pp. 3313–3329.